CHAPTER VIII

TRANSFERABLE EXFOLIATED GRAPHENE OXIDE (eGO) FILMS WITH TUNABLE MICROSTRUCTURES

Chapter Overview

Two investigations of the eGO films prepared by electrophoretic deposition (EPD) were pursued in this chapter. The first investigation was concerned with the microstructure-dependent properties of the films. Recently, one group of researchers showed that the water contact angle of the surface of a drop cast eGO film could be tuned by adding acetone to the aqueous eGO suspension from which the films were drop cast [20]. They attributed the phenomena primarily to the presence of varying amounts of acetone adsorbed to the eGO surface, but also suggested that differences in the films' smoothness could affect the wetting. In the previous chapter, we showed how to use EPD to produce smooth (rug morphology) and bumpy (brick morphology) films from aqueous eGO suspensions. Here, we report on the surface wetting of these films.

The second investigation of the electrophoretically deposited eGO films explored the preparation of free-standing films using the sacrificial layer technique. Cellulose acetate (CA) was selected as the sacrificial layer polymer because it is insoluble in water yet somewhat hydrophilic [12]. Rug and brick eGO films were deposited atop a 110 nm CA layer spun cast on the steel electrodes. The CA layer was dissolved in acetone to liberate the eGO films. The characterization of the free-standing eGO films is reported.

8.1 Wettability of eGO Films

The eGO films were deposited on steel substrates using the parameters outlined in Section 7.3: rug morphology using suspension regime 1 (deposition with 3 V, 15 min) and brick morphology using suspension regime 3 (deposition with 15 V, 10 min). We measured the wettability of the eGO films using a Ramé-Hart contact angle goniometer in the group of Professor Kane Jennings. The advancing and receding contact angles were recorded. The

water contact angle reported here is the advancing contact angle. The contact angle data are shown in Figure 8-1.
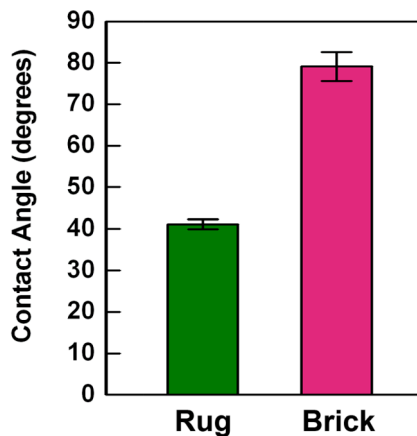

Figure 8-1. Water contact angle of rug and brick eGO films were 41.1° ± 1.2° and 79.1° ± 3.5°, respectively. For comparison, steel substrate contact angle was 77.5° ± 0.7°.

The brick eGO films were considerably more hydrophobic than the rug films. We anticipated that eGO films would be fairly hydrophilic given that eGO could form stable aqueous suspensions. Considering that EPD does not alter the overall chemistry of the colloids being deposited, we attributed the difference in surface wettability to the films' distinct morphologies. Because the manipulation of films and coatings to yield different surface wettability is of immense interest for applications such as anti-fogging and self-cleaning materials, we decided to explore the creation of free-standing rug and brick eGO films. Making these eGO films transferable would enable them to be deployed on a wider selection of substrates.

8.2 Preparation of Free-standing eGO Films

The usefulness of eGO films with different surface wetting behaviors would be multiplied if these films were made free-standing so they could be transferred to arbitrary substrates. To prepare free-standing eGO films, we turned to our sacrificial layer electrophoretic deposition (SLED) method. Cellulose acetate (CA) from Sigma-Aldrich (M_W = 30,000) was selected because it is insoluble in water, and therefore would not dissolve away in the aqueous eGO

suspension. We spun cast the CA onto square pieces of 316L steel (4 cm x 4 cm) from a 10

mg/ml solution in acetone using parameters of 1,000 rpm for 60 s. This yielded a CA layer with

thickness 110 nm. The water contact angle of the CA layer was 54.0° ± 1.2°, in line with

measurements reported in the literature [12]. The CA layer was more hydrophilic than the steel

surface, which had a water contact angle of 77.5° ± 0.7°. Electrodes were cut from the CA-

coated steel (1.5 cm x 3 cm), and a small section of CA was wiped away with an acetone-soaked

swab to ensure a good connection to the EPD circuitry. Depositions were performed using the

parameters outlined in Section 7.3: rug morphology using suspension regime 1 (deposition with 3

V, 15 min) and brick morphology using suspension regime 3 (deposition with 15 V, 10 min). CA-

coated steel was used for the electrode where film deposition would occur while plain steel was

used for the other electrode.

We compared the EPD currents in these experiments to the currents observed when both

electrodes are plain steel. The current did not exhibit any drop-off due to the polymer's presence

(Figure 8-2). For both suspension regimes, the current in this set of experiments was slightly

higher than the current in the previous experiments. We attributed the slight increase in current

to the increased wetting of the CA-coated electrode surface compared to the steel electrode
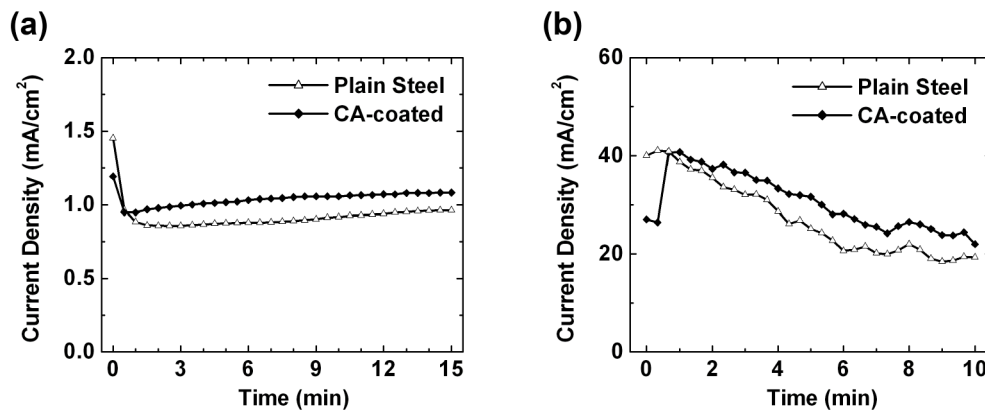
surface.

Figure 8-2. EPD currents (a) for suspension regime 1 and (b) for suspension regime 3 when both electrodes are plain steel and when one plain steel electrode is paired with a CA-coated one.

To separate the eGO films from their substrates, we placed the electrodes in acetone to dissolve the CA polymer. Unlike the nanoparticle films described in Chapter 5, these films did not spontaneously detach from their substrates. The eGO films resisted being fractured by the motion of the underlying polymer because the adhesion between eGO sheets was stronger than the adhesion between the spherical iron oxide nanoparticles, per calculations shown in Chapter 2. To spur the release of the films from their substrate, we pushed a single-edge razor blade along the steel surface while holding it at a nearly parallel orientation to the surface. This maneuver yielded macroscopic film sections floating in the acetone (Figure 8-3).
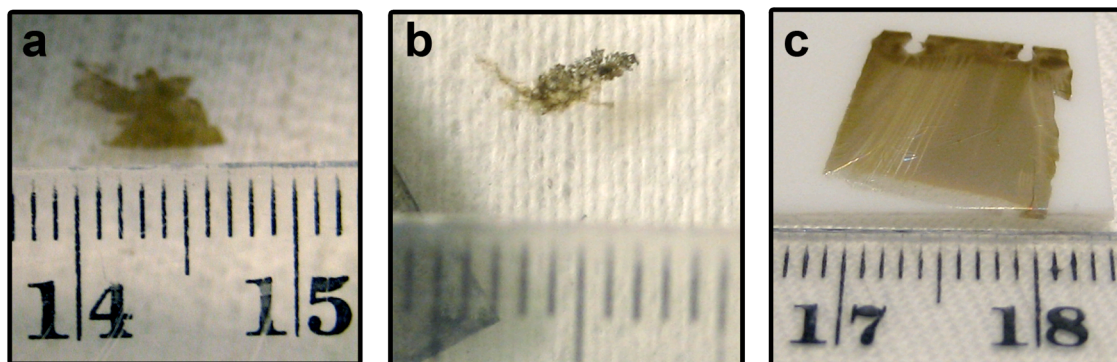

Figure 8-3. Photographs of the free-standing eGO films. (a) Rug and (b) brick films floating in acetone after liberation. (c) Rug film transferred to Teflon sheet. Larger size compared to (a) primarily a function of more adroit razor pushing. The ruler shown in all three frames was demarcated in millimeters, i.e., 10 mm or 1 cm separation between "14" and "15" in (a).

The dimensions of the free-standing rug films were determined primarily by the movement of the razor blade, i.e., whether we could push the blade under a film without slicing the film inadvertently. With a few repetitions, we were able to improve the edge dimensions of the film from ~ 0.5 cm to greater than 1.2 cm, i.e., liberate the entire deposited film intact. The brick films, on the other hand, fragmented at arbitrary locations, with an upper limit of 0.6 cm in its edge dimensions. Additionally, during the liberation of the brick films, sub-millimeter sized film debris was released as well. The release of this debris combined with the spontaneous fragmentation during liberation suggested that the brick film's constituents were not bound together as strongly as the constituents of the rug film. This observation corroborated our

description of the brick film deposition process, in which the eGO sheets formed multilayered stacks prior to reaching the electrode. The multilayered stacks would be larger and more rigid than individual sheets. Therefore, the brick film comprising these stacks would contain more void spaces than the rug film. The presence of void spaces would reduce the surface area in contact between film constituents, thus weakening their adhesion.

In the next section we present morphological characterization of the free-standing eGO films. Contact angle measurements were performed on only the liberated rug films because the area of the brick films was not sufficient for the measurement.

8.3 Characterization of Free-standing eGO Films

The morphology of the free-standing eGO films was examined by scanning electron microscopy (SEM). Some of the films rolled up near their edges, enabling us to image the edges free from substrate interference. These images were used to calculate the thickness of the films. The chemical bonding states in the films were assessed by x-ray photoelectron spectroscopy (XPS). Finally, we did contact angle measurements on liberated eGO rug films which had been transferred to a Teflon substrate.

From the SEM images, we compared the morphologies of the two types of free-standing films. Similarly to what was reported in the EPD survey experiments with eGO, the free-standing brick film appeared more bumpy than the free-standing rug film (Figure 8-4). The free-standing films did not appear identical to their substrate-bound counterparts, likely as a result of infiltration by acetone. From a series of edge images, we were able to calculate the free-standing films' thicknesses. The rug films had thickness 288 ± 18 nm while the brick films had thickness 2,046 ± 283 nm. The large uncertainty associated with the brick films' thickness was reasonable considering that no mechanisms were employed to control the size of the multilayered stacks of eGO sheets that constituted the films.
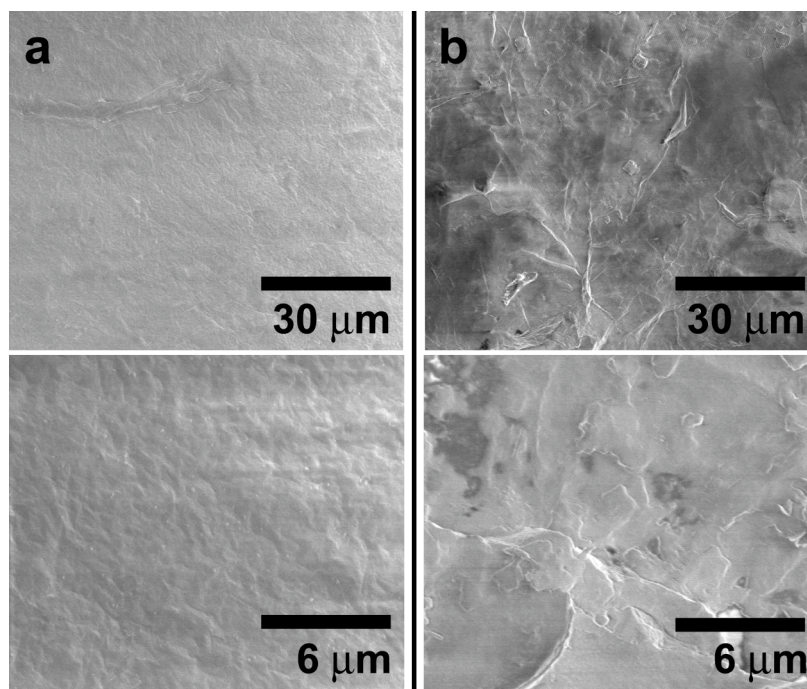
Figure 8-4. Low and high magnification SEM images of the (a) rug and (b) brick eGO films.

We wished to ascertain whether any changes in the chemistry of eGO caused the different wetting behaviors reported in Section 8.1. XPS was employed to compare the chemical bonding states of the rug films to those in the brick films. Free-standing films of each microstructure were transferred to Piranha-cleaned SiO_2 (100 nm on Si) substrates. Figure 8-5 shows survey scans of each film. As anticipated, carbon and oxygen were detected in both films. Unexpectedly, both measurements exhibited signals for zinc. We attributed the presence of zinc to the use of the razor blade during film liberation. Zinc is typically used as an anticorrosion coating for stainless steel objects such as razor blades. Region scans indicating the bonding states for Zn 2p(3/2), O 1s, and C 1s are shown in Figure 8-6. The rug and brick eGO samples appeared to have minimal differences in their chemical bonding states. More importantly, the C 1s scan for both films contains peaks for C–C and C–O bonding, suggesting that the colloidal building block is essentially unchanged after the electrophoretic deposition process. These XPS data present an opportunity for quantitative modeling to determine if the ratio of C to O atoms remains unchanged in the eGO sheets as they go from the starting suspension to the final film.
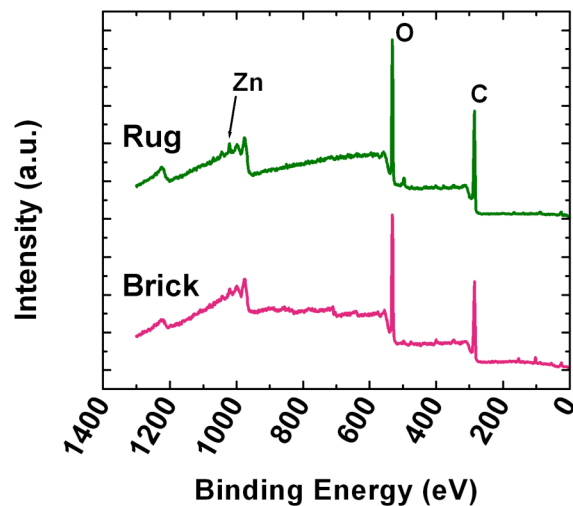
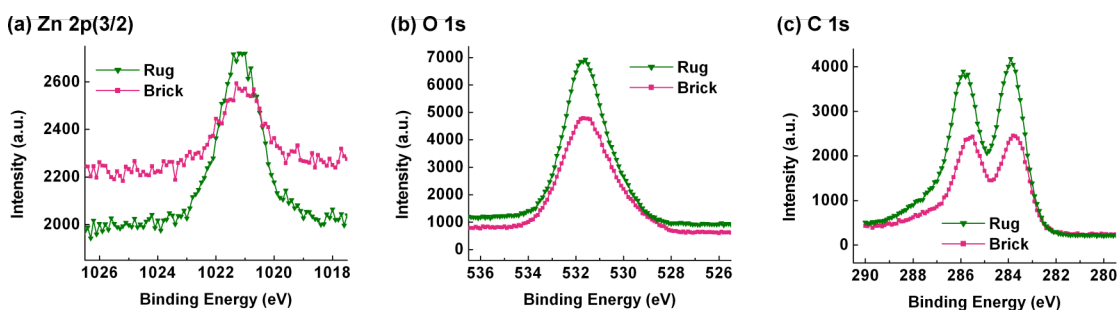Figure 8-5. XPS survey scans of the rug and brick eGO films.

Figure 8-6. XPS region scans of the eGO films showing the (a) Zn 2p(3/2), (b) O 1s, and (c) C 1s bonding states.

We transferred the eGO rug films to a sheet of Teflon to perform contact angle measurements on them. The eGO films had a contact angle of 59.0º ± 1.9º. (As expected, the Teflon substrate was extremely hydrophobic, with a contact angle of 115.5º ± 2.1º.) The eGO rug film resting on Teflon demonstrated lower hydrophilicity than the same type of film prior to liberation. The introduction of wrinkles when resting the film on the Teflon likely caused this change.

With further refinement in the film handling process, and perhaps selection of a different sacrificial polymer and solvent, it may be possible to transfer the eGO rug films to arbitrary locations and retain the low contact angle of the as-deposited film. Despite our rudimentary

handling techniques, the eGO rug films remained intact at lateral dimensions exceeding 1 cm. The relative strength of this film derived from its microstructure, in which individual eGO sheets laid flat over large areas to provide a high surface area for attractive interactions between the sheets. This rug-like microstructure also contributed to the low water contact angle of the films. In contrast, the brick-like microstructure that gave its film a high water contact angle made it a less-than-ideal material to produce as a large-scale free-standing object because the void spaces in the material reduced the surface area for attractive interactions between the film constituents. Still, our SLED technique enabled us to produce free-standing brick eGO films on a macroscopic scale. The findings reported in this chapter validate the broad applicability of the sacrificial layer electrophoretic deposition method to produce free-standing materials solely comprising nanoscale building blocks.

Note: In a discussion after the above content of this chapter was written, Professor Rogers said that the 600-900 eV region of the survey scan of the brick sample indicated the presence of iron and possibly other components of steel. The presence of these elements in the film sample suggested that the steel might have corroded during the deposition from acidic suspension and plated out with the film. To avoid corrosion effects, it would be very interesting to explore the deposition of eGO sheets using corrosion-resistant alloys such as Hastelloy C-22 for the electrodes. This new work will be pursued as an outgrowth from this dissertation. We also note that the possibility of metal ions dissolving into the suspension does not contradict the deposition mechanism proposed in Chapter 7 since the metal ions are positively charged like the H+ ions.